DOI:10.1021/jf102037g

JOURNAL OF AGRICULTURAL AND FOOD CHEMISTRY
ARTICLE

Analysis of Milk Odd- and Branched-Chain Fatty Acids Using Fourier Transform (FT)-Raman Spectroscopy

I. Stefanov,[†] V. Baeten,[‡] O. Abbas,[‡] E. Colman,[†] B. Vlaeminck,[†] B. De Baets,[§] and V. Fievez*,[†]

[†]Laboratory for Animal Nutrition and Animal Product Quality (LANUPRO), Faculty of Bioscience Engineering, Ghent University, Proefhoevestraat 10, B-9090 Melle, Belgium, [‡]Food and Feed Quality Unit, Valorisation of Agricultural Products Department, Walloon Agricultural Research Centre, Chaussée de Namur 24, B-5030 Gembloux, Belgium, and [§]Department of Applied Mathematics, Biometrics and Process Control, Faculty of Bioscience Engineering, Ghent University, Coupure Links 653, B-9000 Ghent, Belgium

Fourier transform (FT)-Raman spectra of pure C13:0, C15:0, C17:0, *iso* C14:0, *iso* C15:0, and *ante* C15:0 fatty acid methyl ester standards (FAMESs) and 75 milk fat samples from 6 different dietary experiments were acquired at room temperature (RT) and immediately after freezing at −80 °C (FT). The latter generally included much more well-defined and sharper scattering bands than those obtained at RT. Further, the spectra at FT revealed additional acuate bands in the vicinity of peculiar wavenumber regions, as well as an increase of Raman scattering intensity, which was sometimes associated with a shift of the peak. Partial least-squares (PLS) regression models based on either selected regions or the full spectra and using two pretreatment methods [multiplicative scatter correction (MSC, using raw spectra of milk fat only) and modified MSC (MMSC, a combination of pure FAMESs and milk fat spectra)] with cross-validation were used to evaluate the different types of milk fat FT-Raman spectra for the predictions of individual odd- and branched-chain fatty acids (OBCFAs) and their sums. In general, most individual (C15:0, *ante* C15:0, *iso* C17:0, and *ante* C17:0) and grouped (ODD, ANTE, and total OBCFAs) fatty acids were favorably (coefficient of determination, $R^2 > 0.65$) predicted using models with FT spectra only or a combination of RT and FT spectra (RFT), when compared to models with spectra analyzed at RT only. The results indicate the interest to use FT-Raman spectra collected at different temperatures for the prediction of narrow concentrations of saturated OBCFAs in milk fat.

KEYWORDS: Raman; spectroscopy; temperature; PLS; MSC; milk fat; fatty acids

INTRODUCTION

To make appropriate nutritional and management decisions on dairy farms, additional tools assessing the nutritional status of a dairy herd, such as milk urea (*1*) or β-hydroxybutyrate (*2*) estimations, are helpful. In earlier studies, we also showed the potential of odd- and branched-chain fatty acids (OBCFAs) for this purpose, e.g., milk secretion of these OBCFAs was related to duodenal flow of microbial biomass (*3*). Further, individual saturated odd-, iso-, and anteiso-branched chain fatty acids (FAs), in particular *iso* C14:0, C15:0, and C17:0, have the potential to monitor the nutrients produced during digestive processes (*4*, *5*). Practical application requires fast determination of these milk OBCFAs. Spectroscopy could be a powerful approach in this respect.

The spectroscopy methods proposed for the analysis of the FAs content in milk or milk fat are infrared (IR) spectroscopy, including mid-infrared (MIR) spectroscopy and near-infrared (NIR) spectroscopy, Raman spectroscopy, and ultraviolet−visible (UV−vis) spectrophotometry. While Raman is one of the less examined spectroscopy techniques, it has recently gained popularity as an excellent tool for the identification and, in some reports, the quantification of molecular constituents (*6*). One of the main reasons for this is the advantage of Raman spectra to exhibit well-resolved bands of fundamental vibrational transitions, thus providing a high content of molecular structure information (*6*). Several studies have used Raman spectroscopy to describe the quality parameters of fats and oils, such as the determination of the oil and water content in olive and olive pomace (*6*, *7*), maturation and authentication of oils and fats (*8*−*11*), as well as the degree of unsaturation of oils and waxes (*12*−*14*), and the quantitative determination of saturated, monounsaturated, and polyunsaturated FAs in lard (*15*). Only a few studies on predictions of milk FAs using Fourier transform (FT)-Raman have been reported (*16*, *17*).

The accuracy in the determination of the FA profiles has been improved via innovations in spectroscopy instrumentation, as well as statistical methodology. However, little attention has been paid to the improvement of the experimental conditions, e.g., the temperature of the sample at the moment of spectra acquisition and its influence on the spectral chemical information. The temperature is

*To whom correspondence should be addressed. Telephone: +32-9-264-90-01. Fax: +32-9-264-90-99. E-mail: veerle.fievez@ugent.be.

 Published on Web 10/01/2010

an analytical condition rarely controlled in major fat and oil analyses based on Raman, MIR, or NIR spectroscopy. Nevertheless, IR spectra of FAs and milk fat have been shown to differ under changing environmental and temperature conditions (*18*, *19*). No similar studies were found on Raman spectroscopy.

The aim of this work was to investigate the potential of Raman spectroscopy to determine OBCFAs in milk fat. In addition, the study investigates the importance of the spectra acquisition temperature conditions and the physical state of the sample during the analysis, as well as its effect on the FA prediction models.

MATERIALS AND METHODS

Sample Selection. A total of 100 milk samples were selected from a sample bank (n = 1033) of six different experiments. The different cow-feeding experiments aimed at changing the FA profile of dairy products. Because of the insufficient number of samples within each experiment to cover the naturally occurring range of OBCFAs, the FA data from the six experiments were combined and used in a mathematical selection method. The subset selection method applied for the selection of the samples is described by Scheerlinck et al. (*20*). Briefly, milk samples were selected on the basis of high, mid, and low concentration ranges of several milk FAs of interest (*iso* C14:0, *iso* C15:0, *iso* C17:0, *ante* C15:0, *ante* C17:0, C15:0, C17:0, and different *trans*-C18:1 and *cis*/*trans*-C18:2 isomers) by optimizing a fitness function using genetic algorithms. The raw milk samples were stored frozen (allowing a long-term preservation) until extraction of the milk fat.

FA Standards. Odd- and branched-chain fatty acid methyl ester standards (FAMESs) C13:0, C15:0, C17:0, *iso* C14:0, *iso* C15:0, and *ante* C15:0 were purchased from Larodan (Larodan Fine Chemicals, Malmo, Sweden).

Extraction Technique. A novel milk fat extraction method was developed and implemented in the routine Raman spectroscopy procedure (*21*). Briefly, 10 g (~0.0001 g) of each raw milk sample was mixed with 16 mL of previously prepared dichloromethane/ethanol (DM/E) solution (2:1 ratio, v/v) in a 40 mL centrifuge-grade glass test tube. The mixture was shaken manually with a vortex (Digital Vortex Mixer, VWR International LLC, Sacramento, CA) for 90 s and then centrifuged for a minimum of 8 min (2500*g* at −4 °C, Beckman J2-21, Fullerton, CA). The upper aqueous phase was carefully removed with a pipet, and additionally, 10 mL of the DM/E solution was added to the test tube. The mixture was further vortexed and then centrifuged for a minimum of 6 min (2500*g* at −4 °C). A small precipitate (containing milk protein) and an upper organic phase containing the milk fat were apparent. The latter was filtered (597 $^1/_2$, 240 mm diameter, Schleicher and Schuell, Dassel, Germany) to a suitable round-bottom flask (250 mL). Dichloromethane was removed using a rotary evaporator (Büchi R-104, Büchi Labor AG, Flawil, Switzerland), and samples were left in a desiccator to evaporate until dryness.

Gas Chromatography (GC) Reference Data. Quantification of FAs and FA groups using spectral data requires precise GC reference data. However, coelution of branched-chain FAs with n number of carbon atoms and unsaturated FAs with $n - 1$ number of carbon atoms may be a problem with the highly polar columns generally used for FA analysis of ruminant milk (*22*, *23*). Here, we used the temperature dependency of the polarity of cyanopropyl phases (*24*) to mathematically deduce concentrations of overlapping FAs using two different temperature programs without prior fractionation. A similar approach was described before (*22*, *25*). After extraction, all samples were methylated (*21*) and fatty acid methyl esters (FAMEs) were analyzed by GC according to Vlaeminck et al. (*3*). (first temperature program) and by an isothermal (T = 180 °C) (second) temperature program. Implementation of both temperature programs without prior separation on Ag^+ thin-layer chromatography (TLC), allowed quantification of OBCFAs, which coelute with specific *cis* or *trans* monounsaturated FAs when only one GC temperature program is used. Because of a different separation with the second temperature program, most FAs could be quantified individually as previously described (*22*) and illustrated in **Table 1** for the current experiment. Because coelution of FAs also depends upon the column status, the identity of the FAs and coeluting peaks regularly requires confirmation by injections of Ag^+ TLC fractions. Due to a limited sample quantity for 8 of the 100 selected samples, GC profile reference data were available for 92 milk fat samples only.

Table 1. Resolution of the Geometric and Positional C16:1 Isomers from Branched C17:0 FAs (FA Clusters 1 and 2), C17:1 Isomers from Branched C18:0 (FA Cluster 3), C18:1 Isomers (FA Cluster 4), and C20:0 from C18:3 *n*-6 (FA Cluster 5)[a]

FA cluster 1	C16:1*t*6/7	C16:1*t*8	C16:1*t*9	*iso* C17:0	C16:1*t*10	C16:1*t*11/12	C16:1*c*7
(A)[b]	1	2	3	4	4	5	5
(B)[b]	1	1	1	1	2	2	3
FA cluster 2	C16:1*c*9		C16:1*t*13		*ante* C17:0		C16:1*c*10
(A)[b]	1		1		2		2
(B)[b]	1		2		2		3
FA cluster 3	*iso* C18:0			C17:1*c*7			C17:1*c*8
(A)[b]	1			1			1
(B)[b]	1			2			3
FA cluster 4	C18:1*t*12	C18:1*c*8	C18:1*t*13/14	C18:1*c*9	C18:1*t*15		C18:1*c*11
(A)[b]	1	1	2	2	3		3
(B)[b]	1	2	2	3	3		4
FA cluster 5	C20:0						C18:3 *n*-6
(A)[b]	1						1
(B)[b]	1						2

[a] The same numbers in a single row indicate coelution. [b] (A) Temperature program as described by Vlaeminck et al. (*3*). (B) Isothermal temperature program at 180 °C.

Raman Spectroscopy. FT-Raman spectra were acquired on a Vertex 70, RAM II Bruker Instruments (Bruker Analytical, Madison, WI) FT-Raman spectrometer, equipped with a Nd:YAG laser (yttrium aluminum garnet crystal doped with triply ionized neodymium) with an output at 1064 nm (9398.5 cm^{-1}). The measurement accessory was prealigned. Only the z axis of the scattered light was adjusted to set the sample in the appropriate position regarding the local point. The 180° backscattering refractive geometry, CaF_2 beam splitter, and liquid-nitrogen-cooled Ge diode detector have been used. The spectrometer was managed through the OPUS for Windows software of Bruker Instruments. The spectral data were obtained with a resolution of 4 cm^{-1} and a nominal laser power of 600 mW. Milk fat and pure FA standards (~0.1−0.3 g) were analyzed in vials selected by CRA-W in previous Raman analysis (*11*) with PE-caps (Klaus Ziemer GmbH, Mannheim, Germany), at room temperature (~25 °C) (RT) and immediately after placing in a freezer at −80 °C for a period of 15 min (FT). To ensure homogenization of the milk fat, all samples were melted at 38 °C in a water bath, at a minimum of 1 h prior to temperature treatment. For each spectrum, 64 scans were co-added and averaged to obtain a good signal-to-noise ratio. A total of 3734 data points were recorded from 0 to 3599 cm^{-1}. Because of very low milk fat quantity in 14 and extraction solvent contamination in 3 of all 92 selected samples, Raman spectroscopy data in RT and FT were available for 75 milk fat samples.

Data Treatment. Standard partial least-squares (PLS) regression was carried out using the Unscrambler, version 9.1 (CAMO, Trondheim, Norway). The pre-processing method of choice was multiplicative scatter correction (MSC), which corrects for variation in spectral scattering intensity. MSC was performed using raw spectra of milk fat only (MSC) or with a combination of pure FAMESs and milk fat (MMSC). The uncertainty testing "jackknife" procedure in the Unscrambler program was used to select variables that correlated with the measured parameter and to reject data from Raman shifts not contributing to the prediction. For all PLS models, validation was carried out using systematic cross-validation with 3 folds and 25 units per segment. The optimal number of PLS factors used for the regression was determined from the minimum residual validation variance. Outliers were detected using residual y-validation variance.

PLS regression was performed according to three different strategies, which differed in the number of predictor variables used (selected spectral regions versus full spectral range) and types of samples used in the MSC

Table 2. Vibrational Bands and Intensities of FAMESs as Obtained from Raman (Bruker RAM II) Spectra at FT after MSC[a]

C13:0		C15:0		C17:0		*iso* C14:0		*iso* C15:0		*anteiso* C15:0	
ν (cm^{-1})	intensity[b]	ν (cm^{-1})	intensity[b]	ν (cm^{-1})	intensity[b]	ν (cm^{-1})	intensity[b]	ν (cm^{-1})	intensity[b]	ν (cm^{-1})	intensity[b]
3019	6	3019	6	3019	3	3019	10	3025	6	3029	14
2950 sh	39	2950 sh	39	2953 sh	15	2952 sh	62	2952 sh	59	2952 sh	63
2925 sh	55	2925 sh	61	2930 sh	24	2930 sh	74	2925 sh	78	2925 sh	80
2882	100	2882	100	2882	100	2885	100	2886	95	2888	96
								2879	98	2879	98
						2868	97	2868	96	2868	97
2850	85	2850	96	2846	61	2850	95	2851	100	2851	100
						2761 s	8	2761 s	6	2760 s	11
2727	9	2727	10	2727	7	2718	14	2717	12	2717	17
1742	6	1742	6	1742	2	1742	6	1739	7	1740	7
1457 b,sh	21	1460 b,sh	19	1462 s,sh	13	1463 s,sh	25	1461 b,sh	23	1462 b,sh	24
						1448	31	1450	28	1450	29
1441	30	1440	30	1441	20	1440	31	1440	31	1440	31
1419 s,sh	10	1419 s,sh	9	1419 s,sh	8						
1370	3	1370	3	1370	2	1371	4	1366	4	1365	5
						1337 s	8	1337 s	7	1336 s	8
1297	20	1296	19	1296	23	1297	18	1297	17	1297	18
1178 b	2	1163 b	2	1175 b	1	1170 s	6	1170 s	5	1168 s	6
1127 s	11	1129 s	8	1130 s	12	1135 s	8	1135 s	6	1134 s	7
1081	7	1081	7	1102	4	1088	8	1081	7	1080	8
1062	12	1062	11	1062	14	1062	10	1063	9	1063	10
						954 s	6	954 s	6	955 s	6
891 s	10	885 s	8	886 s	5	884 s	8	885 s	7	885 s	7
849 b	4	849 b	4			819 s	10	823 s	8	824 s	9
						610 b	2	610 b	2	611 b	3
419 s	5	407 s	2	492 s	2	440 s	5	429 s	4	429 s	6
217 b	4	223 b	5	364 b	2	223 b	6	209 b	5	214 b	7
156 s	13	135 s	14	121 s	20	148 s	11	136 s	11	137 s	12

[a] b, broad vibrational band; s, sharp vibrational band; sh, shoulder band. [b] Intensity in percentage of the maximum peak at 2882 cm^{-1} (C13:0, C15:0, and C17:0), 2885 cm^{-1} (*iso* C14:0), and 2851 cm^{-1} (*iso* C15:0 and *ante* C15:0).

pre-processing model (MSC versus MMSC). For the selected spectral regions, Raman spectra were reduced from 3734 to 1650 variables, by including only regions that are commonly believed to be the carriers of the chemical information (3100−2600 and 1850−750 cm^{-1}) (*11*). PLS|A consisted of using PLSR with MSC and selected scattering regions (1650 variables). PLS|B consisted of using PLSR with MSC and the full Raman spectra (3734 variables). PLS|X consisted of using PLSR with MMSC and the full Raman spectra (3734 variables). In addition, each of the PLS|A, PLS|B, and PLS|X methods were performed for RT only, FT only, and concatenated RT and FT spectra (RFT). A total of 9 prediction models for each of the individual OBCFAs (*iso* C13:0, *ante* C13:0, *iso* C14:0, *iso* C15:0, *ante* C15:0, C15:0, *iso* C17:0, *ante* C17:0, and C17:0) as well as for ODD (sum of C5:0, C7:0, C9:0, C11:0, C13:0, C15:0, C17:0, C19:0, C21:0, and C23:0), ISO (sum of *iso* C13:0, *iso* C14:0, *iso* C15:0, *iso* C16:0, *iso* C17:0, and *iso* C18:0), ANTE (sum of *ante* C13:0, *ante* C15:0, and *ante* C17:0), BRANCHED (sum of ISO and ANTE), and OBCFA (sum of ODD and BRANCHED) FA groups were built.

RESULTS

Spectral Observations. A detailed description of Raman shifts and corresponding Raman intensities from spectra of pure FAMESs derived in FT conditions can be found in **Table 2**. In general, FT-derived spectra of FAMESs revealed additional well-defined Raman scattering bands in the vicinity of 1418, 419, and 156 cm^{-1} (C13:0), 1418, 407, and 135 cm^{-1} (C15:0), 1418, 492, and 121 cm^{-1} (C17:0), 3020, 1063, 439, and 147 cm^{-1} (*iso* C14:0), 3026, 1063, 430, and 137 cm^{-1} (*iso* C15:0), and 3029, 2760, 1064, 955, and 137 cm^{-1} (*ante* C15:0), when compared to RT Raman spectra. Full Raman spectra of pure FAMESs derived in FT and RT conditions can be found in **Figure 1**.

The FT spectra of milk fat showed an increase in Raman scattering intensity in the vicinity of 2890 (shifted to 2880 cm^{-1}), 1747 (shifted to 1740 cm^{-1}), 1438, 1370, 1300 (shifted to 1295 cm^{-1}), 1125, 1062, and 890 cm^{-1}, as well as additional scattering bands in the vicinity of 1727, 1420, 1110, 920, and 605 cm^{-1}. The extent of the latter varied between milk fat samples. Full Raman spectra of one randomly selected milk fat sample derived in FT and RT conditions can be found in **Figure 2** as an example.

FA Composition. An overview of the results from the reference gas chromatographic analyses is presented in **Table 3**. The variation coefficients for all individual OBCFAs and the OBCFA subgroups was on average 21% and varied between 12 and 33%. Minimum and maximum values indicated that the range of OBCFAs naturally occurring in milk fat was covered by the current data set. However, total OBCFAs maximally represent 6 g/100 g of milk fat. The cross-correlation results between the individual FAs and the major FA groups indicated that there was a high correlation ($R^2 > 0.90$) between C15:0 and OBCFA, as well as between C15:0 and ODD.

PLS Results. PLS regression with cross-validation was performed on selected spectral bands (PLS|A) and full-range spectra (PLS|B) using MSC of all milk fat samples ($n = 75$), as well as on full-range spectra using MSC of all milk fat samples with spectra of pure FAMESs (PLS|X). The validation coefficient of determination (R^2), the root-mean-square error of cross-validation (RMSECV, g/100 g of FAMEs), and the number of PLS factors for OBCFA, ODD, BRANCHED, ISO, ANTE, as well as individual C15:0, C17:0, *iso* C13:0, *iso* C14:0, *iso* C15:0, *iso* C17:0, *ante* C13:0, *ante* C15:0, and *ante* C17:0 FAs, are presented in **Table 4**. Intercept, slope, and bias parameters of the best prediction models are presented in **Table 5**. In general, except for C17:0 FA (a R^2 of 0.564 and RMSECV of 0.071 with seven PLS factors), using FT only or a combination of RT and FT (RFT) spectra produced better prediction results compared to RT spectra only. OBCFA and ANTE PLS|B models, using FT and

combined RFT spectra, gave a R^2 of 0.661 and 0.813 and RMSECV of 0.348 and 0.050 using four and seven PLS factors, respectively. Further, except for *iso* C14:0 and *ante* C13:0 FAs, the best individual FA prediction models gave a R^2 above 0.50, with *ante* C17:0, *ante* C15:0, and C15:0 having the best overall parameters: R^2 of 0.795, 0.741, and 0.706 and RMSECV of 0.028, 0.036, and 0.188, using six, seven, and four PLS factors, respectively (**Table 4**).

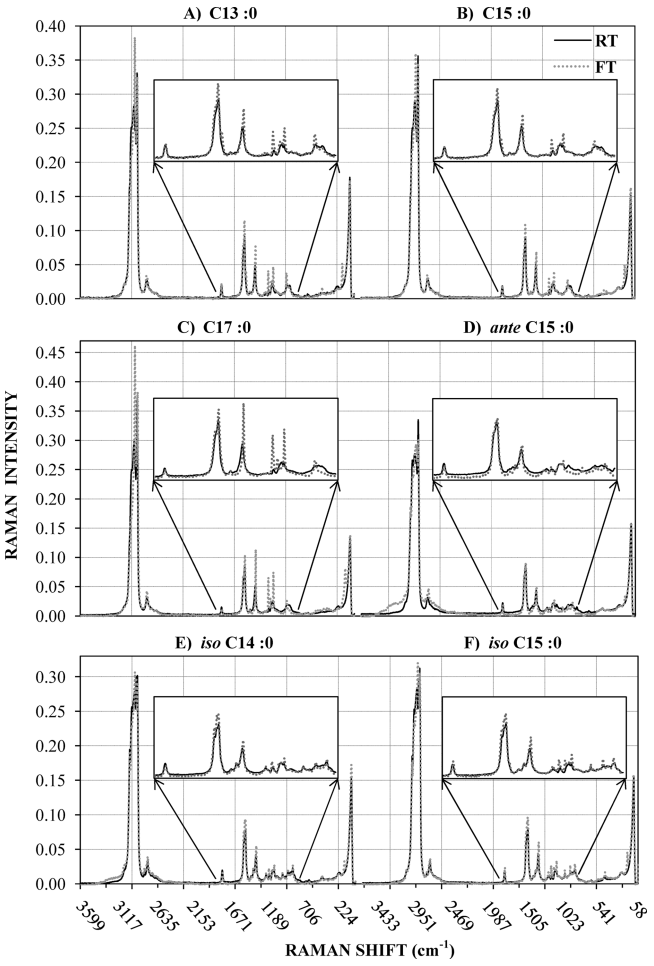

Figure 1. MSC Raman spectra of FT (dotted line, after freezing at −80 °C) versus RT (solid line) for (A) C13:0, (B) C15:0, (C) C17:0, (D) *ante* C15:0, (E) *iso* C14:0, and (F) *iso* C15:0 pure FA standards [*x* axis, wavenumbers (cm^{-1}); *y* axis, scattering intensity].

DISCUSSION

Raman Spectroscopy. Upon analysis of the C17:0 methyl ester standard, it was noticed that its FT-Raman spectrum differed significantly from the FT-Raman spectra of methyl C13:0 and methyl C15:0, when analyzed under RT conditions (~25 °C). Further, the physical state of C17:0 FAMEs at RT was identified as solid, while the C13:0 and C15:0 FAMEs were liquids. The spectral patterns of liquefied FAMESs were fairly broad and diffuse, while the patterns obtained in solid state were generally much sharper, narrower, and with larger Raman scattering intensity (**Figure 1**). The extent of spectral perturbations (increases in scattering intensity, new peaks, and peak shifts) was found to vary with the different FAMESs, and the threshold line of drastic transformations was the sample melting point. Thus, the Raman spectra of the sample obtained during solid physical state might contain additional chemical and/or structural information.

Intensities in the vicinity of 2900−2880, 1747−1740, 1470−1340, 1305−1295, and 1132−885 cm^{-1} regions are known to be related to the methyl C−H symmetric stretching, C═O carbonyl group stretching, CH_2 and CH_3 bending, $-(CH_2)_n-$ in-phase twisting, and C−C stretching vibrational modes, respectively (**Figure 2**). In contrast, there is very little information regarding the additionally observed Raman scattering bands in the 900−200 cm^{-1} region of solidified FAMESs, which could possibly be assigned to the C−C−C skeletal rocking and bending vibrational modes. Further, no information regarding the additionally discovered Raman scattering bands below 200 cm^{-1} was found in the literature (*26*). Hence, it was not possible to attribute the origin of the differences observed in FT-derived spectra of milk fat below 750 cm^{-1} to specific vibrational modes.

There is insufficient information regarding the origin of the stretching vibrations in the 2800−2650 cm^{-1} Raman region. The latter was previously investigated by Lawson et al. (*27*) and found to be characteristic of methyl branching in organic compounds. The feature in the vicinity of 2700 cm^{-1} is normally disregarded and not attributed to any fundamental vibration. A new weaker

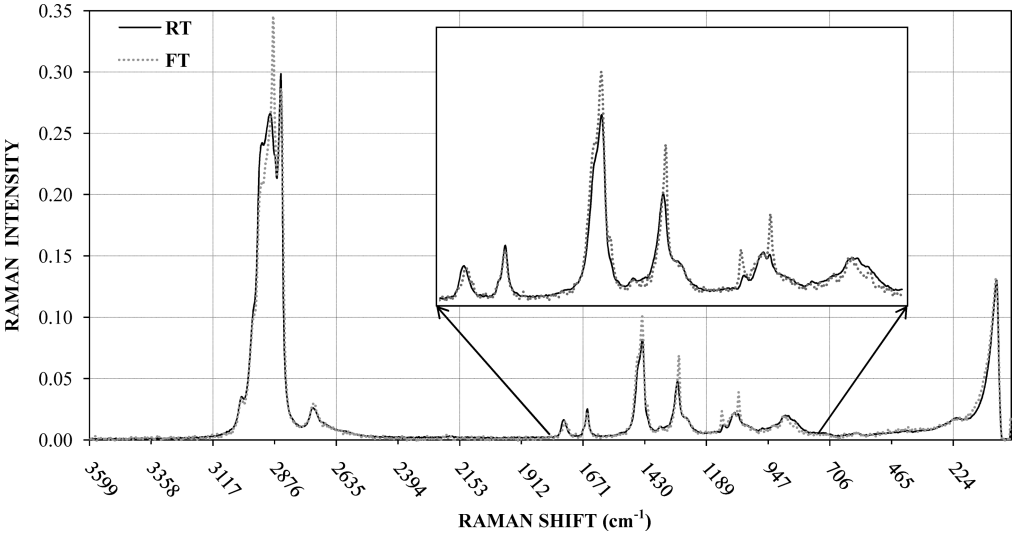

Figure 2. FT (dotted line, after freezing at −80 °C) versus RT (solid line) MSC Raman spectra of a randomly selected milk fat sample, 0−3599 cm^{-1} [*x* axis, wavenumbers (cm^{-1}); *y* axis, scattering intensity].

Table 3. Concentration Range of Saturated Odd, *iso*, and *anteiso* FAs, as Well as the Sum of the Odd (ODD), Branched (BRANCHED), Branched *iso* (ISO), Branched *anteiso* (ANTE), and Total Odd- and Branched-Chain (OBCFA) FA Groups (g/100 g of FAMEs; $n = 75$)

	iso C13:0[a]	*ante* C13:0[b]	*iso* C14:0[a]	*iso* c15:0[a]	*ante* C15:0[b]	C15:0[c]	*iso* C17:0[a]	*ante* C17:0[b]	C17:0[c]	OBCFA[a,b,c]	ODD	BRANCHED[a,b]	ISO	ANTE
minimum	0.012	0.005	0.033	0.116	0.167	0.462	0.155	0.228	0.301	2.34	1.11	1.23	0.572	0.533
maximum	0.048	0.025	0.115	0.283	0.533	2.59	0.467	0.520	0.777	5.94	4.43	2.03	1.10	1.05
average	0.029	0.012	0.068	0.187	0.406	1.44	0.265	0.357	0.434	3.38	1.84	1.54	0.766	0.775
standard deviation	0.008	0.004	0.019	0.027	0.070	0.345	0.054	0.063	0.101	0.597	0.548	0.181	0.100	0.115

[a] Individual FAs reported as well as *iso* C16:0 and *iso* C18:0 are included in the sum of *iso* branched-chain FAs (ISO). [b] Individual FAs reported are included in the sum of *ante* branched-chain FAs (ANTE). [c] Individual FAs reported as well as C5:0, C7:0, C9:0, C11:0, C13:0, C19:0, C21:0, and C23:0 are included in the sum of odd-chain FAs (ODD).

Table 4. PLS Regression Results for Individual OBCFAs and Their Subgroups[a] Using Selected Windows (750−1800 and 2750−3100 cm^{-1}, PLSA) and Full-Range (0−3599 cm^{-1}, PLSB and PLSX) Raman Spectra of Milk Fat Samples Analyzed at RT, FT, and RFT Spectra ($n = 75$)[b]

		RT			FT			RFT		
	OBCFA	PLSA	PLSB	PLSX	PLSA	PLSB	PLSX	PLSA	PLSB	PLSX
C15:0	R^2	0.460	0.611	0.610	0.289	0.670	**0.706**	0.000	0.476	0.489
	RMSECV	0.254	0.219	0.219	0.290	0.199	**0.188**	0.371	0.253	0.245
	number of PLS	6	7	7	3	4	**4**	1	6	4
C17:0	R^2	0.293	**0.564**	**0.564**	0.119	0.091	0.091	0.164	0.428	0.445
	RMSECV	0.085	**0.071**	**0.071**	0.095	0.097	0.097	0.092	0.077	0.076
	number of PLS	3	**7**	**7**	1	1	1	1	3	5
ODD	R^2	0.444	0.296	0.296	0.307	0.585	0.586	0.188	**0.642**	0.188
	RMSECV	0.414	0.464	0.464	0.454	0.352	0.352	0.492	**0.351**	0.360
	number of PLS	6	5	5	2	3	3	1	**9**	7
iso C13:0	R^2	0.154	0.482	0.483	0.003	0.036	0.036	0.081	**0.502**	0.263
	RMSECV	0.007	0.006	0.006	0.008	0.008	0.008	0.008	**0.006**	0.007
	number of PLS	3	6	6	1	1	1	1	**6**	3
iso C14:0	R^2	0.208	0.009	0.009	0.315	0.069	0.069	0.234	0.003	0.003
	RMSECV	0.017	0.020	0.020	0.015	0.018	0.018	0.016	0.020	0.020
	number of PLS	3	1	1	3	1	1	3	1	1
iso C15:0	R^2	0.101	0.080	0.080	0.246	0.020	0.021	0.148	0.394	**0.504**
	RMSECV	0.026	0.026	0.026	0.024	0.027	0.027	0.026	0.022	**0.019**
	number of PLS	4	1	1	3	1	1	2	6	**3**
iso C17:0	R^2	0.447	0.439	0.439	0.533	**0.656**	**0.656**	0.512	0.495	0.498
	RMSECV	0.040	0.041	0.041	0.037	**0.033**	**0.033**	0.038	0.038	0.038
	number of PLS	1	2	2	3	**6**	**6**	3	2	2
ISO	R^2	0.189	0.052	0.054	0.285	0.342	0.342	0.316	0.120	0.123
	RMSECV	0.090	0.097	0.097	0.084	0.081	0.081	0.083	0.096	0.095
	number of PLS	3	1	1	2	4	4	5	3	3
ante C13:0	R^2	0.065	0.263	0.263	0.012	0.429	0.450	0.128	0.205	0.314
	RMSECV	0.004	0.003	0.003	0.004	0.003	0.003	0.004	0.003	0.003
	number of PLS	2	3	3	1	3	4	2	2	4
ante C15:0	R^2	0.307	0.044	0.044	0.329	0.533	0.534	0.707	0.028	**0.741**
	RMSECV	0.061	0.072	0.072	0.064	0.048	0.048	0.039	0.072	**0.036**
	number of PLS	5	1	1	5	3	3	8	1	**7**
ante C17:0	R^2	0.243	0.338	0.337	0.328	0.159	0.159	0.548	**0.795**	0.737
	RMSECV	0.055	0.052	0.052	0.052	0.059	0.059	0.043	**0.028**	0.032
	number of PLS	3	4	4	3	3	3	8	**6**	5
ANTE	R^2	0.173	0.243	0.193	0.343	0.044	0.045	0.637	**0.813**	0.786
	RMSECV	0.110	0.100	0.104	0.092	0.116	0.116	0.070	**0.050**	0.054
	number of PLS	5	3	3	2	2	2	7	**7**	9
BRANCHED	R^2	0.169	0.273	0.274	0.194	0.092	0.092	0.350	**0.701**	0.630
	RMSECV	0.164	0.157	0.158	0.162	0.177	0.177	0.149	**0.100**	0.114
	number of PLS	2	4	4	2	3	3	7	**7**	8
OBCFA	R^2	0.466	0.568	0.575	0.300	**0.661**	0.665	0.319	0.537	0.514
	RMSECV	0.446	0.391	0.388	0.498	**0.348**	0.356	0.490	0.404	0.427
	number of PLS	7	5	5	2	**4**	5	3	3	5

[a] Odd (ODD), branched *iso* (ISO), branched *anteiso* (ANTE), the sum of ISO and ANTE (BRANCHED), and the sum of ODD and BRANCHED (OBCFA) FA groups. [b] Spectra were corrected using MSC either with (PLSX) or without (PLSA and PLSB) including spectra of pure FAMESs (C13:0, C15:0, C17:0, *iso* C14:0, *iso* C15:0, and *anteiso* C15:0). Best results (bold) are based on lowest RMSECV (in g/100 g of FAMEs) and $R^2 > 0.50$.

stretching vibration in the vicinity of 2760 cm^{-1} was observed in the branched-chain FAMESs but not in any of the straight-chain FAMESs (**Figure 3**). This led us to believe that the 2800−2650 cm^{-1} region is indeed related to branching in the saturated FAs, which we investigated here, in agreement with observations for alkanes by Lawson et al. (*27*).

RT versus FT PLS Results. On the basis of the latter spectral observations and the perturbations linked with the physical sample state, we further compared prediction abilities of RT, FT, and a concatenated RT and FT (RFT) FT-Raman spectra of milk fat for the quantification of individual OBCFAs and their subgroups {OBCFA [ODD and BRANCHED (ISO and ANTE)]}.

Table 5. Intercept, Slope, and Bias Regression Parameters of Selected Models for Prediction of Individual OBCFAs and Their Subgroups Using Selected Windows (750−1800 and 2750−3100 cm^{-1}, PLSA) and Full-Range (0−3599 cm^{-1}, PLSB and PLSX) Raman Spectra of Milk Fat Samples Analyzed at RT, FT, and RFT Spectra (n = 75)

	OBCFA	ODD	BRANCHED	ANTE	C15:0	C17:0	*iso* C13:0	*iso* C15:0	*iso* C17:0	*ante* C15:0	*ante* C17:0
model	FT PLSB[a]	RFT PLSB[a]	RFT PLSB[a]	RFT PLSB[a]	FT PLSX[b]	RT PLSX[b]	RFT PLSB[a]	RFT PLSX[b]	FT PLSB[a]	RFT PLSX[b]	RFT PLSB[a]
intercept	0.974	0.342	0.323	0.086	0.251	0.116	0.010	0.090	0.058	0.077	0.061
slope	0.716	0.828	0.792	0.890	0.771	0.749	0.670	0.518	0.780	0.815	0.824
bias	0.013	0.025	0.002	<0.001	0.012	0.007	<0.001	<0.001	<0.001	0.002	<0.001

[a] Using MSC on spectra (0−3599 cm^{-1}) of all 75 milk fat samples. [b] Using MSC on spectra (0−3599 cm^{-1}) of all 75 milk fat samples in combination with spectra of pure C13:0, C15:0, C17:0, *iso* C14:0, *iso* C15:0, and *anteiso* C15:0 FAMEs.

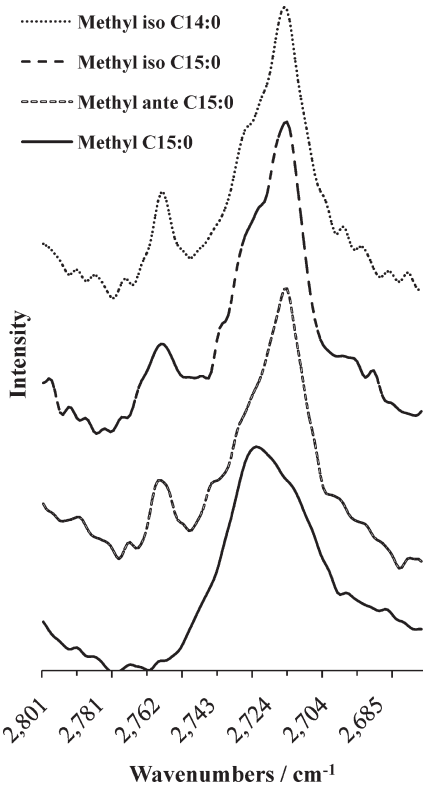

Figure 3. Raman spectra over the wavenumber range of 2800−2670 cm^{-1} of pure branched-chain *iso* C14:0, *iso* C15:0, *ante* C15:0, and straight-chain C15:0 FAMESs [*x* axis, wavenumbers (cm^{-1}); *y* axis, scattering intensity].

In general, using FT or RFT with full spectra and MSC (PLS|B) or in combination with MSC of FAMESs (MMSC) (PLS|X) models produced significantly better prediction results for all FA groups, as well as for all individual FAs, except for C17:0, when compared to models using spectra of samples analyzed at RT (**Table 4**). Prediction models for C15:0 with FT spectra produced good results, with PLS|X having the best model parameters (**Table 4**). Similarly, using FT produced the best models for the OBCFA group. The latter could be an indication of the influence from the individual C15:0 FA in the OBCFA predictions. A comparable prediction behavior of C15:0 and OBCFA should not be surprising, taking into account the high correlation (R^2 = 0.90) between their reference data. Thus, predictions of OBCFA are most likely largely determined by C15:0. The Unscrambler regression coefficient plot from the C15:0 PLS|X model for FT indicated significant Raman shifts in the vicinity of 1256, 1287, 290, 316, 1532, 678, 2177, and 2565 cm^{-1} (listed in order of decreasing regression coefficient). In addition to the latter variables determining the calibration model of C15:0, other essential variables influence the prediction of OBCFA (e.g., 2960, 857, 2938, 1040, and 1697 cm^{-1}). Regression coefficients for the ODD PLS|X model using FT were similar to the best C15:0 model (possibly because of the very high correlation between their reference data; R^2 = 0.96), although the best ODD prediction model (a R^2 of 0.642 and RMSECV of 0.351 with nine PLS factors) was with concatenated RFT spectra. The latter could be an indication of the influence from the better C17:0 results with RT, thus when RT and FT spectra are combined, the ODD model improves. Prediction models of C17:0 using the full spectra at RT showed significantly better results, when compared to all FT and RFT models (**Table 4**). The latter should be taken into serious consideration, because of the fact that the spectral information, which is contained in the RT-derived spectra, is still present in RFT combined spectra but not teased out during the PLS regression procedure with the "jackknifing" variable selection method; thus, inclusion of overwhelming information could be counterproductive. The Raman shifts from the regression coefficient plot of the Unscrambler, which contributed the most in the determination of the best C17:0 models, were in the vicinity of 1636, 1657, and 162 cm^{-1}.

Predictions models for the *ante* C15:0 and *ante* C17:0 FAs, as well as for the ANTE FA group had the best model parameters when compared to all other individual and group FA models. In addition, the contrast between the results of the RT and FT models with *ante* C15:0 might indicate that the FT spectra contain additional chemical information, which would help to improve the predictions. Using RFT gave R^2 of 0.741 and RMSECV of 0.036 for the *ante* C15:0 PLS|X model and even better results ($R^2 \geq 0.80$) for the *ante* C17:0 and ANTE PLS|B models. A similar prediction behavior of both individual FA and the ANTE FA group should not be surprising, because these FAs represent 98% of ANTE and, hence, are highly correlated (*ante* C15:0 + *ante* C17:0 and ANTE; $R^2 > 0.99$). The Unscrambler regression coefficient plot from the *ante* C17:0 PLS|B model for RFT indicated significant Raman shifts in the vicinity of 3012, 861, 3063, 750, 1328, and 768 cm^{-1} (listed in order of decreasing regression coefficient). The latter also appeared as significant shifts in the regression coefficient plot of the best ANTE prediction model. The regression coefficient plot of the best *ante* C15:0 PLS|X model showed significant Raman shifts in the vicinity of 1638, 1259, 48, 1072, 3011, and 98 cm^{-1}.

Overall, prediction results for the individual and group ISO FAs were poor, with the exception of *iso* C17:0 predictions. Higher prediction results for *iso* C17:0 compared to any other of the *iso* FAs is striking, and we feared this could have been caused by partial coelution with *trans*-10 C16:1 during GC, despite the precautions taken to avoid this, i.e., analysis by two different temperature programs (**Table 1**). However, concentrations of both FAs as determined by GC analysis showed no correlation (R^2 = 0.03). Predictions of *iso* C15:0 using RFT produced moderate results, while none of the *iso* C13:0 and *iso* C14:0 models produced satisfactory results (**Table 4**).

Poor predictions for *iso* C13:0 and *iso* C14:0, as well as for the *ante* C13:0 FA, could be due to the very low concentration of the FAs in the milk fat (**Table 3**). At such low quantities, it would be a strenuous task to extract chemical information about the variations in these FAs, even with an information-rich spectroscopy technique, such as Raman.

Full Spectra versus Selected Windows. In general, using the full spectra (PLS|B) provided a significant improvement in the predictions of all individual FAs and all FA groups, with the exception of *ante* C15:0. The RFT partial spectra (PLS|A) model of the latter gave better parameters when compared to PLS|B, and higher numbers of PLS components were required (**Table 4**). These results could indicate that the PLS regression in the Unscrambler, combined with the "jackknifing" uncertainty variable selection method, was in that case lacking the ability to extract the information, which was originally contained in the PLS|A model. Other variable selection methods and/or raw spectra processing techniques should be investigated for the improvement in extraction of the chemical information from the spectra.

Raman Spectra Variations. Milk fat crystallization and melting processes are known to be very complex (*28*, *29*). The latter is due to the wide range of triacylglyceride compositions, which leads to a broad melting point of the milk fat sample, spanning from about −40 to +40 °C (*30*). In this regard, apprehending the relationship between the sample molecular composition and the molecular behavior, which causes changes in the spectra under different temperature conditions, is a powerful tool in understanding spectral behavior.

The raw Raman spectra signal analyzed at FT was found to be less intense (∼2−4-fold lower scattering intensity) compared to the raw RT spectra. The latter could be attributed to (1) the lower ground energy of the sample molecules in solid state compared to the ground energy in liquid state and/or (2) the formation of a crystal lattice in milk fat, which could result in the backscattering of most incident light photons (with energy and wavenumber equal to those of their incident ones), and hence, only a small portion of all light photons is allowed to enter in the periodic crystal structure (*31*). In addition, smaller variations in the scattering intensity of the spectra in samples analyzed under the same temperatures (RT or FT) were observed. The latter is a common observation in raw spectra and could be attributed to slight variations in the laser source.

MSC versus MMSC Pre-processing. The variations in Raman scattering intensity were corrected using a MSC technique, a commonly used pre-processing method for spectroscopic data. Although MSC has been established as an important tool for removing unwanted variability, there could be a tendency for information in one part of the spectrum to be shifted elsewhere or simply smeared across the whole wavelength range (*32*). The limitation of MSC is that it uses the mean spectra of all observations as a reference value; thus, some of the chemical information contained in the spectra might be diminished (*33*). To prevent the loss of subtle spectral variations, it should be ensured that samples with spectra corrected using the same MSC model are analyzed under the same spectroscopy method parameters. An alternative solution for keeping more chemical information, suggested by Sayes et al. (*33*), could be adding the spectra of pure components of interest (in our case, pure FA standards) during the spectra pre-processing step (MMSC). In general, using MMSC in PLS models with full-range spectra (PLS|X) improved prediction results for C15:0 using FT-analyzed spectra, as well as *iso* C15:0 and *ante* C15:0 in RFT-derived models (**Table 4**). The lack of improvement for other regression models could indicate that the reference chemical information, which is to be included in the pre-processing step, should reflect the product of prediction interest. In other words, for improvement of ODD FA models, spectra of pure saturated odd-chain FAs only should be included, and for improvement of ANTE FA models, spectra of pure *ante* branched-chain FAs only should be included, etc. In the current assessment, the spectra of all available pure standards were included in any of the MMSC prediction models. The importance of the inclusion of specific FAMESs is the subject of further research.

In conclusion, Raman spectroscopy analysis in combination with a fast milk fat extraction procedure could already be used to address direct routine applications for the quantification of several OBCFAs. Careful choice and control of the experimental conditions are necessary for reproducibility and interpretability and assessing the origin of the information contained in the milk fat spectra; hence, temperature-regulating equipment seems essential. Moreover, the selection of signal pre-processing methodology was found to play an important role and could significantly influence prediction results. The pre-processing method of choice should be able to preserve most chemical information, which was originally contained in the raw spectra.

While the questions of what is the exact pathway under which temperature conditions influence Raman scattering intensities and why it affects only specific Raman shifts still remain and need to be addressed to further increase prediction performance, FT-Raman spectra collected at different temperatures have shown interest to improve predictions of low concentrations of saturated OBCFAs in milk fat.

ACKNOWLEDGMENT

Analyses on Raman spectroscopy as reported are obtained in collaboration with researchers of the Walloon Agricultural Research Centre, Quality Department (head: Pierre Dardenne) within the framework of the collaborative agreement between Lanupro and the Quality Department (A08-TT-0384). Authors thank Alejandro Rodriguez for the technical support.

LITERATURE CITED

(1) Peterson, A.; French, K.; Russek-Cohen, E.; Kohn, R. Comparison of analytical methods and the influence of milk components on milk urea nitrogen recovery. *J. Dairy Sci.* **2004**, *87*, 1747−1750.

(2) Oetzel, G. Monitoring and testing dairy herds for metabolic disease. *Vet. Clin. North Am.: Food Anim. Pract.* **2004**, *20*, 651−674.

(3) Vlaeminck, B.; Dufour, C.; Van Vuuren, A. M.; Cabrita, A. M. R.; Dewhurst, R. J.; Demeyer, D.; Fievez, V. Potential of odd and branched chain fatty acids as microbial markers: Evaluation in rumen contents and milk. *J. Dairy Sci.* **2005**, *88*, 1031−1041.

(4) Vlaeminck, B.; Fievez, V.; Cabrita, A. R. J.; Fonseca, A. J. M.; Dewurst, R. J. Factors affecting odd- and branched-fatty acids in milk: A review. *Anim. Feed Sci. Technol.* **2006**, *131*, 389−417.

(5) Vlaeminck, B.; Fievez, V.; Tamminga, S.; Dewhurst, R. J.; Van Vuren, A.; De Brabander, D.; Demeyer, D. Milk odd- and branched-chain fatty acids in relation to the rumen fermentation pattern. *J. Dairy Sci.* **2006**, *89*, 3954−3964.

(6) Muik, B.; Lendl, B.; Molina-Dıaz, A.; Ayora-Canada, M. J. Direct, reagent-free determination of free fatty acid content in olive oil and olives by Fourier transform Raman spectrometry. *Anal. Chim. Acta* **2003**, *487*, 211−220.

(7) Muik, B.; Lendl, B.; Molina-Dıaz, A.; Perez-Villarejo, L.; Ayora-Canada, M. J. Determination of oil and water content in olive pomace using near infrared and Raman spectrometry. A comparative study. *Anal. Bioanal. Chem.* **2004**, *379*, 34−41.

(8) Baeten, V.; Meurens, M.; Morales, M. T.; Aparicio, R. Detection of virgin olive oil adulteration by Fourier transform Raman spectroscopy. *J. Agric. Food Chem.* **1996**, *44* (8), 2225−2230.

(9) Baeten, V.; Pierna, J. A. F.; Dardenne, P.; Meurens, M.; Garcıa-Gonzalez, D. L.; Aparicio-Ruiz, R. Detection of the presence of

hazelnut oil in olive oil by FT-Raman and FT-MIR spectroscopy *J. Agric. Food Chem.* **2005**, *53* (16), 6201−6206.
(10) Baeten, V.; Aparicio, R. Edible oils and fats authentication by Fourier transform Raman spectrometry. *Biotechnol., Agron., Soc. Environ.* **2000**, *4* (4), 196−203.
(11) Abbas, O.; Fernandez Pierna, J. A.; Codony, R.; Von Holst, C.; Baeten, V. Assessment of the discrimination of animal fat by FT-Raman spectroscopy. *J. Mol. Struct.* **2009**, 294−300.
(12) Sadeghi-Jorabchi, H.; Wilson, R. H.; Belton, P. S.; Edwards-Webb, J. D.; Coxon, D. T. Quantitative analysis of oils and fats by Fourier transform Raman spectroscopy. *Spectrochim. Acta, Part A* **1991**, *47* (9/10), 1449−1458.
(13) Baeten, V.; Hourant, P.; Morales, M. T.; Aparicio, R. Oil and fat classification by FT-Raman spectroscopy. *J. Agric. Food Chem.* **1998**, *46* (7), 2638−2647.
(14) Barthus, R.; Poppi, R. J. Determination of the total unsaturation in vegetable oils by Fourier transform Raman spectroscopy and multivariate calibration. *Vib. Spectrosc.* **2001**, *26* (1), 99−105.
(15) Olsen, E. F.; Rukke, E.; Flatten, A.; Isaksson, T. Quantitative determination of saturated-, mono-unsaturatedand poly-unsaturated fatty acids in pork adipose tissue with non-destructive Raman spectroscopy. *Meat Sci.* **2007**, *76*, 628−634.
(16) Meurens, M.; Baeten, V.; Yan, S. H.; Mignolet, E.; Larondelle, Y. Determination of the conjugated linoleic acids in cow milk fat by Fourier transform Raman spectroscopy. *J. Agric. Food Chem.* **2005**, *53* (15), 5831−5835.
(17) Bernuy, B.; Meurens, M.; Mignolet, E.; Larondelle, Y. Performance comparison of UV and FT-Raman spectroscopy in the determination of conjugated linoleic acids in cow milk fat. *J. Agric. Food Chem.* **2008**, *56* (4), 1159−1163.
(18) Azizian, H.; Kramer, J. K. G.; Winsborough, S. Factors influencing the fatty acid determination in fats and oils using Fourier transform near-infrared spectroscopy. *Eur. J. Lipid Sci. Technol.* **2007**, *109*, 960−968.
(19) Woodrow, I. L.; deMan, J. M. Polymorphism in milk fat shown by X-ray diffraction and infrared spectroscopy. *J. Dairy Sci.* **1957**, *51*, 756−766.
(20) Scheerlinck, K.; De Baets, B.; Stefanov, I.; Fievez, V. Subset selection from multi-experiment data sets with application to milk fatty acid profiles. *Comput. Electron. Agric.* **2010**, *73* (2), 200−212.
(21) Stefanov, I.; Vlaeminck, B.; Fievez, V. A novel procedure for routine milk fat extraction based on dichloromethane. *J. Food Compos. Anal.* **2010**, DOI: 10.1016/j.jfca.2010.03.016.
(22) Kramer, K. J.; Hernandez, M.; Cruz-Hernandez, C.; Kraft, J.; Dugan, M. Combining results of two GC separations partly achieves determination of all *cis* and *trans* 16:1, 18:1, 18:2 and 18:3 except CLA isomers of milk fat as demonstrated using Ag-ion SPE fractioning. *Lipids* **2008**, *43*, 259−273.
(23) Vlaeminck, B.; Harynuk, J.; Fievez, V.; Marriott, P. Comprehensive two-dimensional gas chromatography for the separation of fatty acids in milk. *Eur. J. Lipid Sci. Technol.* **2007**, *109* (8), 757−766.
(24) Mjøs, S. A. Identification of fatty acids in gas chromatography by application of different temperature and pressure programs on a single capillary column. *J. Chromatogr., A* **2003**, *1015* (1−2), 151−161.
(25) Martin, C. A.; de Oliveira, C. C.; Visentainer, J. V.; Matsushita, M.; de Souza, N. E. Optimization of the selectivity of a cyanopropyl stationary phase for the gas chromatographic analysis of trans fatty acids. *J. Chromatogr., A* **2008**, *1194* (1), 111−117.
(26) Socrates, G. *Infrared and Raman Characteristic Group Frequencies*, 2nd ed.; Wiley Publishing: Hoboken, NJ, 2009; pp 14−58.
(27) Lawson, E. E.; Edwards, H. G. M.; Johnson, A. F. FT Raman spectroscopic study of the wavenumber region 2800−2630 cm^{-1} of selected organic compounds. *Spectrochim. Acta, Part A* **1995**, *51*, 2057−2066.
(28) Sherbon, J. W. Crystallization and fractionation of milk fat. *J. Am. Oil Chem. Soc.* **1974**, *51*, 22−25.
(29) Lopez, C.; Lavigne, F.; Lesieur, P.; Bourgaux, C.; Ollivon, M. Thermal and structural behavior of milk fat. *J. Dairy Sci.* **2001**, *84*, 756−766.
(30) Martini, S.; Herrera, M. L.; Hartel, R. W. Effect of cooling rate on nucleation behavior of milk fat−sunflower oil blends. *J. Agric. Food Chem.* **2001**, *49*, 3223−3229.
(31) Landsberg, G.; Mandelstam, L. Uber die licht zerstreuing in kristallen. *Z. Phys.* **1928**, *50*, 769−780.
(32) Davies, T.; Fearn, T. Something has happened to my data: Potential problems with standard normal variate and multiplicative scatter correction spectral pre-treatments. *Spectrosc. Eur.* **2009**, *6*, 15−19.
(33) Sayes, W.; Beullens, K.; Lammertyn, J.; Ramon, H.; Naes, T. Increasing robustness against changes in the interferent structure by incorporating prior information in the augmented classical least-squares framework. *Anal. Chem.* **2008**, *80*, 4951−4959.

Received for review May 29, 2010. Revised manuscript received August 31, 2010. Accepted September 9, 2010. The Ph.D. research of Ivan Stefanov is supported by the Institute for the Promotion of Innovation by Science and Technology in Flanders (IWT) (IWT-PhD-project 60704).